

Slow molecular dynamics close to crystal surfaces during crystallization of a protein lysozyme studied by fluorescence correlation spectroscopy

S. Tanaka^{a)}

Graduate School of Integrated Arts and Sciences, Hiroshima University, 1-7-1 Kagamiyama, Higashi-Hiroshima 739-8521, Japan

(Received 24 February 2010; accepted 20 July 2010; published online 7 September 2010)

Fluorescence correlation spectroscopy (FCS) was applied to the crystallization processes of egg-white lysozyme. Utilizing FCS's high spatial resolution of about the laser wavelength used, the molecular dynamics close to crystal surfaces was investigated for both tetragonal single crystals and needlelike spherulites. When the FCS measurement was done at the point closer than 1 μm to the surface of a tetragonal single crystal, the relaxation time became several times longer than that in bulk solution, but the fluorescence intensity (thus concentration) was similar to that observed in bulk solution. On the other hand, the peculiar slow dynamics (a few orders of magnitude slower than that in bulk solution) of concentrated liquid states of the lysozyme molecules was observed in needlelike spherulites. We suggested that these observations could be explained by the formation of softly connected aggregates accumulating around the needlelike crystals, which could cause the instability of the crystal growth and thus the formation of spherulites. These aggregates gradually disappeared as the crystallization further proceeded. After the disappearance of the aggregates, the spherulites started to mature. © 2010 American Institute of Physics. [doi:10.1063/1.3478224]

I. INTRODUCTION

Protein crystallization is an essential process to determine the three-dimensional structure of proteins with the x-ray crystallography. However, it is often a bottle neck of the process of structure determination because of the complex phase behaviors of protein solutions along with crystallization, which include liquid-liquid phase separation,¹⁻⁵ random aggregation,^{6,7} and gel or glass formation.⁸ A characteristic feature of the protein solutions is that these phase behaviors are often observed as metastable and nonequilibrium.^{6,9} When the solutions are brought into a supersaturated state, phase transitions take place toward the most stable state, which is usually realized as an equilibrium state between a single crystal and a dilute solution. However, the supersaturated solutions are sometimes trapped in metastable states, which prevents further phase transformation. It is not a rare case in protein solutions that they cannot escape from these metastable states and the crystallization never occurs. Therefore, understanding the properties of these metastable or nonequilibrium states is important for the control of the phases in protein solutions.

Among these nonequilibrium states seen in protein solutions, probably one of the most troublesome states is the polycrystallization. Although large and flawless single crystals are needed for the x-ray crystallography, proteins often crystallize in the form of clusters of thin plates, rods, or needles.¹⁰ When these clusters become spherical, they are called spherulites.^{4,5,11} Since the surface area of the spherulites is much larger than that of single crystals, the spherulites are a form of nonequilibrium states, where protein molecules fail to relax into the more stable single-crystal state.

To create single crystals while avoiding polycrystallization, a fine tuning of the crystallization condition, often with trial-and-error approach, is usually necessary and takes time, which makes the crystallization a bottle neck of the whole process of the structure determination.

We have been interested in the formation of spherulites in protein lysozyme solutions.^{4,9} They tend to appear after the liquid-liquid phase separation, and the interplay between spherulite formation and liquid-liquid phase separation makes complex patterns in solutions.⁹ Recent study showed that the liquid-liquid phase separation was not a prerequisite, and a dilute solution was enough to create spherulites.⁵ The liquid-liquid phase separation, which creates a solution of dilute protein with dense salt, seems to be advantageous for spherulite formation. This suggests that the diffusion of molecules plays an important role in the spherulite formation. Similar tendency of the spherulite formation has been observed in a variety of systems.¹²

The branching of a crystal, which is a premise for the spherulite formation, has been studied intensively.¹³ One of the most successful theoretical explanations is Mullins-Sekerka instability.¹⁴ For this instability, there needs to be a field with a gradient where crystals can grow faster if they reach deeper into the gradient. Such a field can destabilize the flat surface and a fluctuation of the surface above a certain wavelength is enhanced, which eventually promotes the branching. So far, it is unclear whether this kind of instability plays a role in the protein spherulite formation.

In this study, therefore, we measured the molecular dynamics close to crystal surfaces to investigate the mechanism of the spherulite formation using fluorescence correlation spectroscopy (FCS). The FCS has several advantages over more commonly used dynamic light scattering (DLS), which

^{a)}Electronic mail: shinpei@hiroshima-u.ac.jp.

include a spatial resolution as high as the optical limit (about the wavelength of light used). Moreover, the fluorescence intensity directly provides information about the local concentration in the position measured. Using FCS, we measured the molecular dynamics in the vicinity of single crystals and in spherulites. The dynamics measured for the two types of crystals was then compared to elucidate what determined the crystal morphology. To our knowledge, this is the first attempt to use FCS for the study of protein crystallization mechanism.

We used lysozyme as a model protein. Many studies have shown that the crystallization behaviors seen in a lot of other proteins can be recognized in lysozyme crystallization.^{10,15} For example, liquid-liquid phase separation in lysozyme solutions, which has been thoroughly studied so far,^{1,3-5} is considered to be a phenomenon which should occur commonly in other protein solutions. Spherulitic crystallization is also observed in a lot of protein solutions.¹¹ Thus, lysozyme is a good model system for at least the study of the phase behaviors during crystallization, and the properties found there can be considered to be a representative of those of many other protein solutions.

II. EXPERIMENTS

A. Materials

Six-times crystallized hen egg-white lysozyme was purchased from Seikagaku Corp., Tokyo, and used without further purification. A proper amount of lysozyme solution and that of sodium chloride were mixed to prepare solutions of the appropriate concentration. All solutions contained 50 mM sodium acetate buffer, and pH was adjusted at 4.5. When the concentrations of lysozyme and sodium chloride were high so that the solution exhibited the liquid-liquid phase separation, it was centrifuged with the speed of 6000 rpm for 2 min. Then the supernatant was used for the further measurements.

A 2 μl sample solution was transferred onto a square cover slip (35 mm) and sandwiched with a round cover slip (15 mm in diameter). The rim of the upper cover slip was sealed with paraffin oil. The thickness of the sample thus prepared was about 3 μm .

Fluorescently labeled lysozyme was made using a dye Alexa-Fluor 488 5-SDP ester (Molecular Probes, USA). The dye was dissolved in dimethylformamide and added to a lysozyme solution. The solution was mixed gently at 4 °C for the reaction. Unreacted dye molecules were then removed by thorough dialysis against water and using a desalting column PD-10 (GE Healthcare, Tokyo) with the molecular weight cutoff of 5000. The degree of labeling was determined by measuring the absorbance of the solution at 280 and 494 nm. The number of dye per protein molecule was about 0.1, which assured the labeled lysozyme molecules have only one dye molecule attached to their surface. The concentration of labeled lysozyme in a sample was fixed at 1 nM.

B. Fluorescence correlation spectroscopy

FCS is a method to detect a number fluctuation of molecules in a laser focus, from which information of the molecular dynamics at the point is obtained.¹⁶ The laser beam is focused into a point whose size can be as small as about the wavelength used ($\sim 0.5 \mu\text{m}$). Though molecules in a solution cannot be directly observed optically, their dynamics can be detected by FCS. Then the structure of the solution can be considered using the information of molecular dynamics. One of the advantages of FCS over DLS is that it can measure dynamics with the spatial resolution of the wavelength used. Thus, we can get information at a specific point, for example, on a surface of a crystal.

FCS measurement was done by a confocal microscope Eclipse TE2000-E (Nikon, Tokyo) equipped with a photon counting module (Hamamatsu Photonics, Shizuoka). An objective lens of oil-immersion type [100 \times , numerical aperture (NA) 1.25] was used. The size of confocal aperture was set to be 100 μm . The light source was a 20 mW solid-state laser (Melles Griot, Tokyo) of the wavelength λ of 488 nm. The theoretical optical (xy -) resolution of the system is calculated as $0.61\lambda/\text{NA}=238 \text{ nm}$. Experimentally, the size of the beam waist s was measured using fluorescent molecules with known diffusion coefficient and assuming¹⁶

$$s^2 = 4D\tau, \quad (1)$$

where D is the diffusion coefficient and τ is the relaxation time obtained from FCS measurements as described below. Rhodamin 6G ($D=400 \mu\text{m}^2/\text{s}$) (Ref. 17) was used for calibration in this study. The value of s thus measured was 240 nm. The z -resolution is determined by the size of a confocal aperture, although it is larger than the cell thickness in this study.

The signal was collected via a digital counting board (National Instruments, Tokyo) and the autocorrelation functions were calculated using LABVIEW (National Instruments). The sampling rate was fixed at 0.1 MHz.

During the measurement, the temperature was controlled by an air conditioner of the room at $20 \pm 1 \text{ }^\circ\text{C}$. This crude way to control the temperature was adopted since the immersion oil connecting the objective lens and the sample cover slip made the sample temperature coincide with that of the microscope.

C. Data analysis

If fluorescent particles in solution are monodispersed, the autocorrelation function measured by FCS is often approximated as¹⁶

$$g(t) = 1 + a_0 \left(1 + \frac{t}{\tau}\right)^{-1} \left(1 + \frac{t}{\tau'}\right)^{-1/2}, \quad (2)$$

where a_0 is the correlation intensity, τ is the diffusion time of the particles in the direction perpendicular to the laser beam, and τ' is the one parallel to the beam. In our setting, however, the sample thickness (about 3 μm) was close to the height of the laser focus thus the particle diffusion parallel to the laser beam was not important. Then we can assume that only two-dimensional diffusion is detected and $g(t)$ becomes,

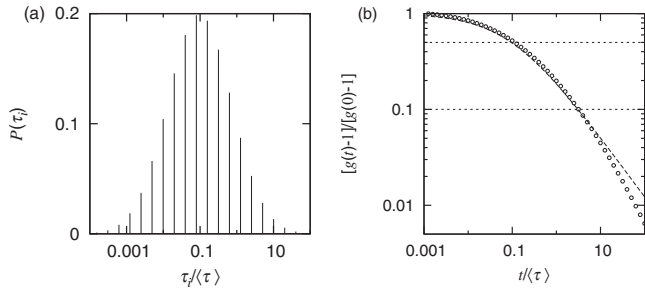


FIG. 1. An artificially made, logarithmically broad distribution $P(\tau)$ of relaxation time τ (a) and the autocorrelation function $g(t)$ (circles) (b) constructed from $P(\tau)$ according to Eq. (4) for the test of the fitting function Eq. (5). The x -axis is normalized by the averaged relaxation time $\langle\tau\rangle$. The result of the fitting is shown by a dashed curve. The dotted lines in (b) show a half and one tenth of $g(0)$ where τ and $\tau_{1/10}$ are defined.

$$g(t) = 1 + a_0 \left(1 + \frac{t}{\tau}\right)^{-1}. \quad (3)$$

Our system contains heterogeneity in diffusion time originating from various reasons such as interaction, aggregation, and so forth. In a polydispersed system $g(t)$ is written as a sum of each relaxation term,

$$g(t) = 1 + \sum_i a_i \left(1 + \frac{t}{\tau_i}\right)^{-1}, \quad (4)$$

where a_i and τ_i are, respectively, the correlation intensity and the diffusion time of the i th term.

In practice, however, the deconvolution of $g(t)$ into many power-law-decay terms is difficult. Thus we use an empirical function form

$$g(t) = 1 + a_0 \left\{1 + \left(\frac{t}{\tau}\right)^\beta\right\}^{-1}, \quad (5)$$

where β is introduced to represent the deviation from a simple power-law decay, which can reflect a broad distribution of τ . Note that the parameter β is often used in a stretched exponential function, where it presents a distribution of the relaxation rates. In this way, we can reduce the number of fitting parameters significantly.

Figure 1 shows a test of the fitting function. A $g(t)$ [circles in Fig. 1(b)] was calculated according to Eq. (4) as a sum of 18 relaxation terms with a logarithmically broad distribution $P(\tau_i)$ shown in Fig. 1(a), as a rather extreme example. That is, if we deconvolute the $g(t)$ exactly, we need 36 fitting parameters (a_i and τ_i) to fit. In Fig. 1, the x -axis is normalized by the averaged relaxation time $\langle\tau\rangle$. The fitting using Eq. (5) is shown by a dashed curve in Fig. 1(b). It is clear that the fitting function Eq. (5) with only three fitting parameters reproduces the $g(t)$ very well. The τ obtained in this fitting is 0.095, which coincides with the peak position of $P(\tau_i)$. The β was 0.63. It is noted that the time at which $g(t)$ relaxes to the half value of $g(0)$ corresponds to the obtained τ . Moreover, the time at which $g(t)$ relaxes to the 1/10 of the value of $g(0)$, denoted by $\tau_{1/10}$ hereafter, corresponds to a value in the tail of $P(\tau_i)$ at the higher end. We use both τ and $\tau_{1/10}$ to express the characteristics of the distribution of relaxation time.

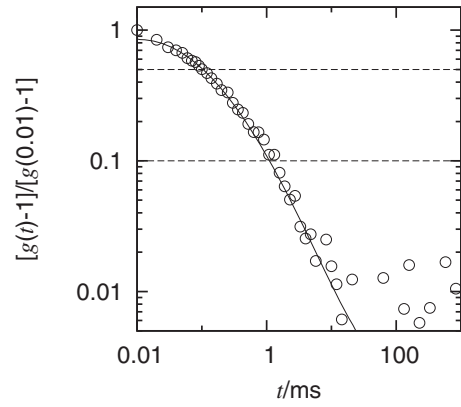


FIG. 2. An autocorrelation function measured (circles) for a dilute (1.0 mg/ml) solution of lysozyme without NaCl. The solid curve is the fitting result using Eq. (5) with $\beta=1$. The relaxation time obtained was $\tau=0.13$ ms. The diffusion coefficient estimated from τ was $110 \mu\text{m}^2/\text{s}$. The corresponding hydrodynamic radius was 2.0 nm.

D. Optical microscopy

All images of the crystallization behaviors were taken by the same microscope used for FCS with a transmittance detector either in a bright field mode or a polarized mode. In polarized microscopy, used for needlelike spherulites in this study, only crystalline domains with optical anisotropy are detected. The images taken with the polarized mode were further Fourier-transformed using an image processing program, ImageJ, with an algorithm of fast Fourier transform (FFT). The obtained FFT images were then radially integrated to produce the structure factor $S(k)$ where k is the wave number.

To obtain the characteristic size of crystal domains, ξ , we assumed a random distribution of the size of crystal domain so that ξ can be obtained as the correlation length. This crude approximation was found to be enough to extract the characteristic size of crystal domains in our samples. Then $S(k)$ was fitted by the Lorentzian

$$S(k) = a_0 / (1 + k^2 \xi^2), \quad (6)$$

where a_0 was a constant.

III. RESULTS

A. Diffusion in bulk solution

First, we show the relaxation of lysozyme molecules diffusing in a bulk, dilute solution (1.0 mg/ml) measured by FCS. Figure 2 shows the autocorrelation function with a fitting. The β was fixed at the unity. The relaxation time was $\tau=0.13$ ms. The diffusion coefficient calculated and the corresponding hydrodynamic radius were, respectively, $D=110 \mu\text{m}^2/\text{s}$ and $r_H=2.0$ nm, which agree well with the previously reported values.¹⁸ It is probably worth mentioning that the concentration of lysozyme can be lowered much further in FCS measurement than DLS since the fluorescence improves the signal-to-noise ratio significantly. This is a salient advantage over DLS when the property in dilute state is of interest. Actually, we found that the diffusion coefficient became significantly larger than the expected value when the

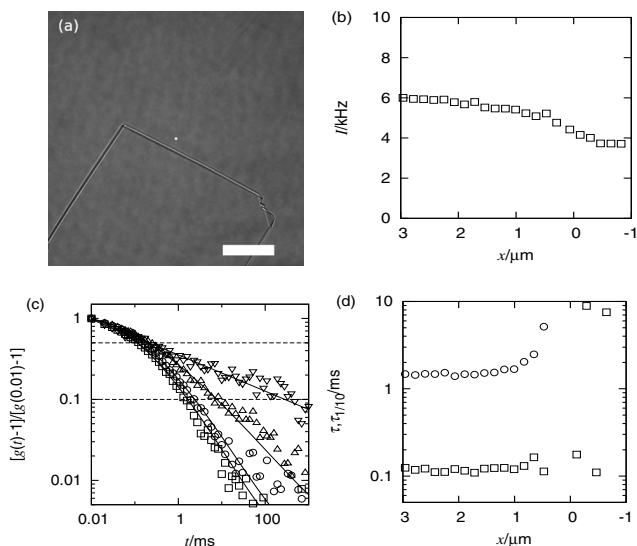


FIG. 3. FCS measurements done close to the surface of a tetragonal single crystal. (a) A bright field micrograph of a crystal and the position of the measurement (the white dot at the center). The scale bar is $20 \mu\text{m}$. This crystal grew at the rate of $5.0 \mu\text{m/h}$ during the measurement, so the crystal surface slowly approached the position of the measurements. (b) The change of the fluorescence intensity depending on the distance x between the laser focus and the crystal surface. (c) The autocorrelation functions taken at the distance of $3.7 \mu\text{m}$ (squares), $0.8 \mu\text{m}$ (circles), $0.5 \mu\text{m}$ (upper triangles), and $0.1 \mu\text{m}$ (lower triangles) from the crystal surface. The dashed lines are drawn to show the $1/2$ and $1/10$ relaxations of the autocorrelation functions. (d) The change of the relaxation times τ (squares) and $\tau_{1/10}$ (circles).

solutions were further diluted, possibly due to the coupling with the motion of small ions as previously observed using DLS.¹⁹ In this study, however, we will not pursue this topic further.

B. FCS at the surface of a single crystal

Figure 3 shows FCS measurements close to the edge of a tetragonal single crystal grown in a solution of 50 mg/ml lysozyme and $0.8M$ NaCl. The position of the laser focus is shown in Fig. 3(a) with a white dot at the center. The size of the dot is roughly the size of the focus. In this picture, the distance between the focus and the crystal surface was about $3.7 \mu\text{m}$. The growth rate at the time of the measurements was $5.0 \mu\text{m/h}$. In the measurements, the focus position was fixed and the crystal surface approached it slowly.

The position dependence of fluorescence intensity I , autocorrelation function $g(t)$, and relaxation time τ are respectively plotted in Figs. 3(b)–3(d). Fluorescence intensity did not change much depending on the position, only slight decrease was seen at the position less than about $1.0 \mu\text{m}$ from the crystal surface. The autocorrelation functions also changed when the position became less than about $1.0 \mu\text{m}$. There appeared a long-time tail in $g(t)$, and the closer to the surface, the longer the tail became. This behavior is represented by β which became much less than unity, and is also well illustrated with τ (squares) and $\tau_{1/10}$ (circles), as shown in Fig. 3(d). $\tau_{1/10}$ was calculated as $\tau_{1/10} = 9^{1/\beta} \tau$, which represents the decay time at which $g(t) - 1$ decays one tenth of $g(0) - 1$. Thus, the smaller the β is, the longer the $\tau_{1/10}$ becomes. It can be seen in Fig. 3(d) that τ did not change much while $\tau_{1/10}$ became longer when the focus was close to the

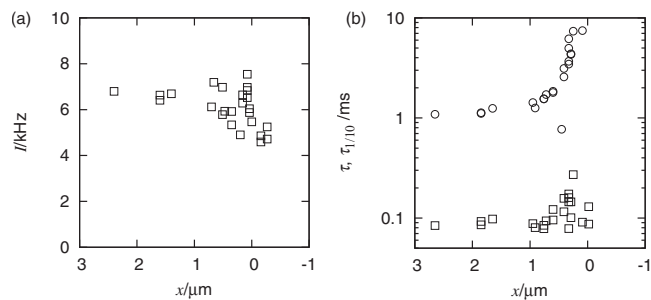


FIG. 4. FCS measurements done using the same solution as those in Fig. 3 but 2 weeks after the sample preparation. The solution has almost reached the equilibrium. (a) The change of the fluorescence intensity. (b) The change of the relaxation times τ (squares) and $\tau_{1/10}$ (circles).

surface. Inside the crystal, that is, at $x < 0$, the fluorescence was bleached rapidly and the measurement of dynamics was not possible. The decay time for the bleach in a crystal was about 40 s .

Similar measurement was done about 2 weeks after the nucleation, so that the crystal has almost reached equilibrium with its surroundings and did not grow during the measurement. In this measurement, the position dependence could be measured in more detail by scanning the focus position since the surface of the crystal did not move. Figure 4 shows the results, which are similar to those shown in Fig. 3. That is, the fluorescence intensity did not depend on the position much, and $\tau_{1/10}$ grew longer when the focus was brought close to the surface.

C. FCS in a needlelike spherulite

Figure 5 shows the FCS measurements done for a needlelike spherulite, grown in supernatant of a solution containing 50 mg/ml lysozyme and $1.6M$ NaCl. The elapsed time of the crystallization, t_m , was measured from the time of mixing solutions. At $t_m \approx 1 \text{ h}$, the growth rate of the spherulite was about $250 \mu\text{m/h}$, though the precise measurement was difficult for the ambiguity of the boundary of the spherulite. Moreover, unlike the measurement for single crystals, the distance between the laser focus and the crystal surface could not be measured for the needlelike morphology of the crystals whose thickness was less than optical resolution at the tip. It was confirmed by microscopy, however, in the initial stage of the measurement around $t_m \sim 0.5 \text{ h}$, the focus did not overlap any crystals. This can be seen in Fig. 5(b) where the fluorescence intensity was low ($\sim 2 \text{ kHz}$) at $t_m \sim 0.5 \text{ h}$. This intensity was the same as that obtained before nucleation took place. Therefore, this value of the intensity was considered to be that in bulk solution.

In $0.5 < t_m < 1 \text{ h}$, the fluorescence intensity increased about ten times, which was attributed to the newly grown crystals entering continuously in the laser focus. This increase of the intensity stopped at $t_m \approx 1 \text{ h}$, then it decreased to the level several times larger ($\sim 8 \text{ kHz}$) than the original value. This decrease indicated that the laser focus was occupied by the needles, and that entering of new needles stopped, since molecules fixed in a crystal are bleached rapidly. This bleach was seen in $1 < t_m < 2 \text{ h}$, then the intensity started to fluctuate around 8 kHz in $2 < t_m < 20 \text{ h}$. The rea-

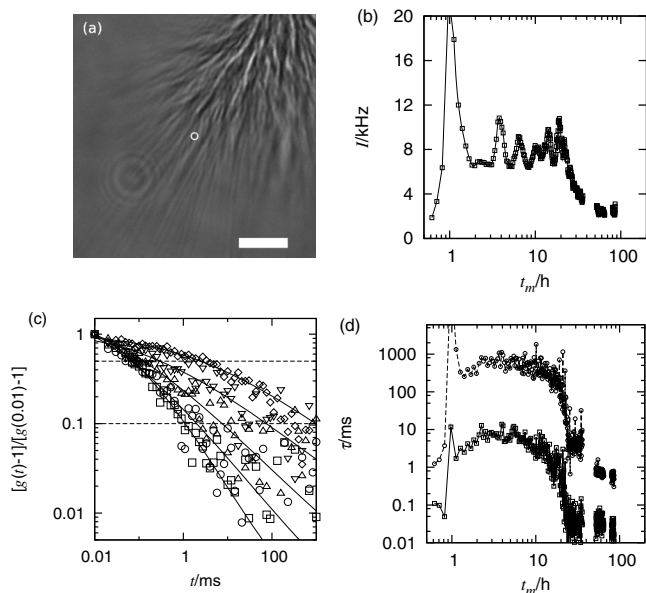


FIG. 5. FCS measurements done in a needlelike spherulite. (a) A bright field micrograph of a spherulite taken at $t_m=0.8$ h. The scale bar is $4 \mu\text{m}$. The position of the laser focus is presented by a circle whose size is approximately the size of the focus. The focus was gradually filled with the needlelike crystals with the growth of the spherulite in a time scale of an hour. (b) The change of the fluorescence intensity. (c) The autocorrelation functions taken at $t_m=0.6$ h (squares), $t_m=0.7$ h (circles), $t_m=0.8$ h (upper triangles), $t_m=1.1$ h (lower triangles), and $t_m=7.5$ h (diamonds). The dashed lines are drawn to show the $1/2$ and $1/10$ relaxations of the autocorrelation functions. (d) The change of the relaxation times τ (squares) and $\tau_{1/10}$ (circles).

son of the seemingly periodic fluctuation was not clear, but it was probably the effect of temperature fluctuation, which was as large as ± 1 °C. In $t_m > 20$ h, the intensity gradually decreased and reached the value of the bulk solution at about $t_m \sim 50$ h.

The peculiar behavior of the intensity was that even after the needlelike crystals filled in the laser focus, the laser did not bleach the entire fluorescence, but the intensity level remained several times higher than the one in the bulk solution. The high fluorescence intensity, which was not bleached suggests that there were concentrated, but still liquidlike (mobile) structure in between needlelike crystals. This will be discussed in detail later.

The autocorrelation functions obtained during the crystal growth are shown in Fig. 5(c). They exhibited a long-time tail like those in Fig. 3(c), but their entire shape was different. This can be seen clearly in the relaxation times obtained by fitting. The relaxation times τ and $\tau_{1/10}$ extracted from the fitting are shown in Fig. 5(d). The points in $t_m < 1$ h in Fig. 5(d) indicated the same relaxation time as those in bulk solution. Then in $t_m > 1$ h, not only $\tau_{1/10}$ but also τ increased with the increase of the fluorescence intensity. This behavior is different from the one seen in Fig. 3(d) and Fig. 4(b), where only $\tau_{1/10}$ increased appreciably.

As shown in Fig. 5(d), τ increased almost two orders of magnitude, whereas $\tau_{1/10}$ increased almost three orders of magnitude from the values in bulk during $1 < t_m < 20$ h. This suggests that the diffusion of molecules were slowed significantly in between needlelike crystals. Still, the lack of bleach also indicates that these slowly moving molecules were not fixed but were in a liquid state.

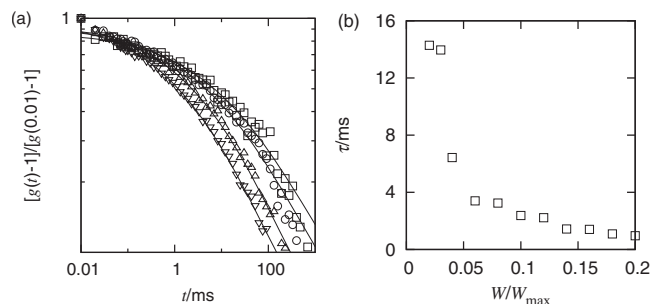


FIG. 6. (a) The effect of bleach on autocorrelation functions. Laser power used was 2% (squares), 4% (circles), 6% (upper triangles), and 14% (lower triangles). The measurements were done in a needlelike spherulite. (b) The effect of the laser power on τ .

These characteristic behaviors, however, began to disappear from around $t_m=20$ h. At about $t_m=50$ h, the fluorescence intensity and the relaxation time reached eventually the values same as those in bulk solution. This means that at this point, there were only molecules diffusing as they were in bulk solution.

D. Effect of bleach

As the bleach is not avoidable for measurements using fluorescence especially when the diffusion of molecules is slow, we checked if it affected the relaxation time extracted from the autocorrelation functions. Figure 6 shows autocorrelation functions measured in a spherulite with different laser power. As shown in Fig. 6(a), the lower the laser power was, the longer the tail of autocorrelation functions became. The effect is also seen in Fig. 6(b). The τ decreased with the increase of the laser power though the effect tended to be saturated at the higher power. Based on this result and considering the signal-to-noise ratio, we chose the laser power $W/W_{\text{max}}=0.05$ for all the measurements, where $W_{\text{max}}=20$ mW was the maximum power of the laser. The τ obtained using this laser power, therefore, should be considered as the lower limit, and the actual relaxation time could be longer than experimentally determined τ .

E. Change of the internal structure of spherulites

Figure 7 shows polarized micrographs of the internal structure of a spherulite obtained during its crystallization process. The micrographs were taken at about the center of

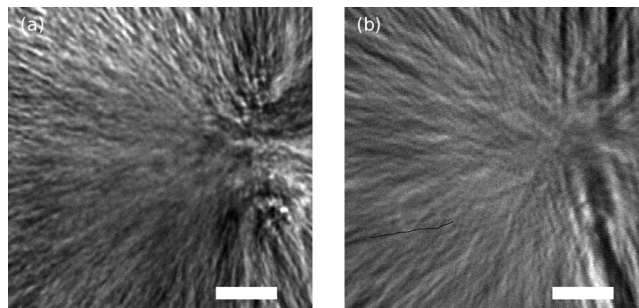


FIG. 7. Polarized micrographs of a spherulite taken at $t_m=1.5$ h (a) and at $t_m=92$ h (b). The scale bar is $4 \mu\text{m}$. The texture was changed, which suggested that the fine structure of the spherulite was matured.

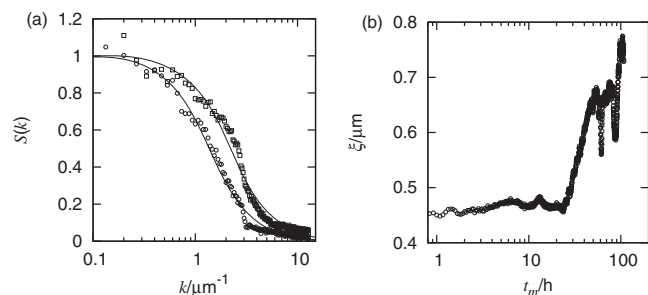


FIG. 8. The results of FFT analysis. (a) The structure factor calculated by radial integration of the FFT images measured at $t_m = 1.5$ h (squares) and at $t_m = 92$ h (circles). The solid curves represent Lorentzian fittings. (b) The Change of the correlation length obtained from the fitting.

the spherulite, whereas its growth occurred mainly at the rim of the spherulite. However, the texture observed at $t_m = 1.5$ h [Fig. 7(a)] was different from that observed at $t_m = 92$ h [Fig. 7(b)]. Since polarized microscopy under the condition of crossed polarizers detects only crystal domains with a certain orientation, the difference in the observed texture indicated that the crystalline structure in the spherulite reorganized during its crystallization process.

To see the change of the internal structure shown in Fig. 7 quantitatively, these micrographs were Fourier-transformed and their radial profiles were calculated, as shown in Fig. 8(a). The profiles shown were calculated from the same micrographs shown in Fig. 7. The profiles were then fitted by the Lorentzian [solid curves in Fig. 8(a)] to extract the correlation length. The wave number of the decay clearly decreased while crystallization proceeded, as shown in Fig. 8(a).

The extracted correlation length ξ is plotted in Fig. 8(b). The values of ξ were consistent with the size of crystal domains shown in Fig. 7. In the initial process ($t_m < 20$ h) ξ was almost constant around $0.45 \mu\text{m}$. Then it increased up to about $0.8 \mu\text{m}$. This increase continued for more than 100 h. These results suggested that the crystals in the spherulite grew to mature and that the maturation started at $t_m \approx 20$ h. Before that, the internal structure of the spherulite did not change for about 20 h. It should be noted that the time when the maturation started almost coincided with the time when the fluorescence intensity and the relaxation time obtained by FCS started to decrease toward the values of bulk solution (Fig. 5).

IV. DISCUSSION

A. Tetragonal single crystals

Fluorescence intensity decreases close to the surface (less than $1 \mu\text{m}$) of tetragonal single crystals when the crystal is growing, as shown in Fig. 3(b). Now we consider the possibility of depletion of molecules around the surface, which can cause the decrease of the fluorescence intensity. The diffusion coefficient of a lysozyme molecule at 20°C is $D \approx 110 \mu\text{m}^2/\text{s}$.¹⁸ Therefore, the root mean squared displacement for 1 s is $\sqrt{\langle \Delta r^2 \rangle} = \sqrt{6D \cdot 1} \approx 26 \mu\text{m}$. This is much larger than the length scale where we observed the decrease in fluorescence intensity. Note that one FCS measurement takes 60–300 s. On the other hand, in this measurement the

crystal surface moved at the rate of $V = 5 \mu\text{m}/\text{h}$. The diffusion length²⁰ is then estimated as $D/V \sim 80 \mu\text{m}$, which is much larger than the system size. Thus, it is concluded that lysozyme molecules are moving much faster than crystal growth rate, so that the depletion of the molecules due to the crystal growth is highly unlikely. Actually, this decrease can be seen close to the surface even in equilibrium, as shown in Fig. 4(a).

If we assume, on the other hand, that the fluorescent molecules fixed in a crystal are bleached rapidly, and that there is no or little concentration inhomogeneity in solution, this decrease can be simply explained by the decrease of the illuminated volume of solution. That is, when the laser focus is brought close to the surface, a part of the focus becomes occupied by the crystal, which decreases the volume of illuminated solution, only where fluorescent molecules can survive and glow. In fact, as shown in Figs. 3(b) and 4(a), the decrease becomes evident when the distance between the focus and the surface becomes less than $1 \mu\text{m}$, whereas the width of the focus is about $0.5 \mu\text{m}$. The results shown in Figs. 3(b) and 4(a), therefore, suggest that there are no or little inhomogeneity in concentration close to the surface of crystals.

The molecular dynamics, on the other hand, is changed when the molecules are near the tetragonal surface. As shown in Fig. 3(c), the autocorrelation functions $g(t)$ have a long-time tail if measured closer than $1 \mu\text{m}$ to the surface. The relaxation time [Figs. 3(d) and 4(b)] extracted from the $g(t)$ shows that $\tau_{1/10}$ becomes several times longer than the value far from the surface, whereas the usual relaxation time τ does not change much. This result suggests that there exist slowly diffusing molecules in addition to the normal molecules near the surface. Their mobility is at least several times lower than those in bulk solution. We consider that these slow molecules either diffuse two dimensionally on the surface or repeat to stick on and off the surface, or both.

It has been shown by several authors that single crystals of lysozyme^{21–23} and other proteins¹⁰ grow with the general crystallization mechanisms,²⁴ such as two-dimensional nucleation and growth, or spiral growth with screw dislocations. These growth mechanisms involve the primary processes on the surface where molecules diffuse two dimensionally and stick to steps or kinks. Our picture is consistent with these surface processes observed on single crystals of various proteins.

The mobility of lysozyme molecules on the surface of tetragonal single crystals in equilibrium has been recently measured by Sasaki and co-workers²⁵ using the method of single-molecule direct imaging. They observed that the number density on the surface was three orders of magnitude larger than the one in a layer of one molecule thickness in the bulk solution. They also observed the diffusion coefficient four to five orders of magnitude smaller than the one in bulk solution. In our method, however, molecules moving too slowly are bleached thus are not detected. It is considered that the molecules they observed are regarded as the molecules fixed in the crystal in our method because of the bleach. Our results suggest that there are much more quickly moving molecules than those observed by Sasaki *et al.*,

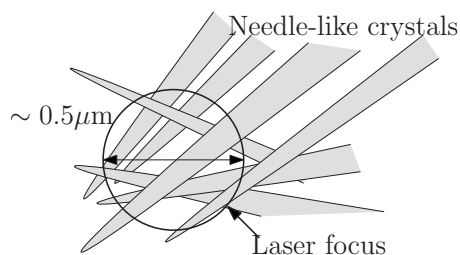


FIG. 9. A schematic drawing of the situation at the focus after needlelike crystals fill the focus.

probably above the surface layers they observed. These molecules are still slower than those in bulk solution. The direct imaging method cannot detect these molecules or molecules in a solution since they are moving too quickly. Therefore, each method provides us different information around the crystal surface and should be considered as complementary.

B. Needlelike spherulites

From Fig. 5(a), the typical width of the needles is less than $1 \mu\text{m}$, and likely more than $0.1 \mu\text{m}$ since they can be recognized optically and the large size of a molecule (about 4 nm in diameter). After the laser focus is occupied by the needles, the situation in the focus is like the one schematically presented in Fig. 9; there are still spaces for solution in between needles.

First, we discuss the initial increase of the fluorescence intensity [Fig. 5(b)]. In the period of $t_m = 0.5 \sim 1 \text{ h}$, needles continuously arrive at the focus, and the growth fronts of the needles (tips) pass through it. Since the growth rate of the spherulite is about $250 \mu\text{m/h}$ in this stage, a needle passes the focus within about 10 s . The fluorescent molecules fixed in a crystal are bleached rapidly with the decay time of less than 1 min , but if the rate of arrival of new needles exceeds the bleach, the fluorescence intensity will increase. If, for example, around three needles pass the focus in a minute, about 100 needles occupy the focus in 30 min . The steep decrease in the fluorescence intensity appears next ($t_m = 1\text{--}2 \text{ h}$) is likely due to the bleach of molecules in needles, which means that the focus is occupied by the needles and the supply of new needles finishes already in this stage.

The peculiar behavior seen in the fluorescence intensity is that the fluorescence is not completely bleached but remains in fairly high values ($6\text{--}8 \text{ kHz}$), which actually several times higher than that in bulk solution ($\sim 2 \text{ kHz}$). The relaxation time in this stage, at the same time, becomes a few orders of magnitude longer than the one observed in bulk solution, which is seen as a steep jump of τ and $\tau_{1/10}$ in Fig. 5(d) at $t_m = 0.8\text{--}1 \text{ h}$. A combination of these two facts suggests that there are fluorescent molecules concentrated at least several times higher concentration than the one in bulk solution, and that they are not fixed in a crystal but are diffusing a few orders of magnitude more slowly than molecules in bulk solution. This state of high fluorescence intensity and long relaxation time continues for about 20 h .

Let us consider here if this state leads to additional aberration of the beam which could expand the laser focus.

First, needlelike crystals did not affect the signal judging from the fact that the intensity and relaxation time decreased to reach the level of bulk solution after a long time as discussed below where needlelike crystals still existed. Next, regarding the concentrated molecules, if we assume the concentration as unrealistically high as 50% , the refractive index increase is only about 0.1 .²⁶ This small increase does not expand the laser focus necessary to explain the increase of I and τ . Thus we can assume that the laser focus was not affected by the presence of these molecules.

These slow and concentrated molecules then start to disappear at around $t_m = 20 \text{ h}$; both the fluorescence intensity and the relaxation time start to decrease. Eventually, they reach the same level as those observed in bulk solution at about $t_m > 50 \text{ h}$. At this stage, therefore, the space in between needles is occupied by molecules same as in bulk solution.

Now let us discuss about the observed state of high concentration of slow molecules. First we consider the molecules slowly and (quasi) two dimensionally diffusing in a layer on the surface of crystals. This kind of layers on the surface is often called add layer. The add layer of lysozyme tetragonal single crystals has been actually observed by Sazaki *et al.*²⁵ as mentioned above. Though this add layer is not observed on the surface of tetragonal single crystals in this study, it is possible to be observed on the needles if their add layer has a higher concentration than that on the single crystals.

The anisotropy of the needles comes from the anisotropy of kinetic coefficients of the growth. It is considered that molecules are not incorporated easily to the side surface of the needles. Since the amount of the needle tips in the focus is relatively small in comparison with that of their side surface (Fig. 9), the high concentration state observed should exist on the side surface. If the concentrated state of the molecules we observed is a sort of add layer, molecules in this add layer should not be incorporated into the crystal while diffusing there.

Next, as another plausible model probably not very different from the add layer model mentioned above, we can consider a dense liquid state of molecules existing around the needles (not necessarily “on” the surface), which can explain our experimental results. We note that stable or metastable dense liquid phase has been observed in protein solutions^{1–4} and its relevance to the crystal nucleation has been discussed,^{27,28} although the relation between the liquid state here and the one observed macroscopically is not clear.

We assume that they form softly connected aggregates for the attraction between molecules. This kind of aggregates can exist in general in protein solutions since a large entropic barrier to form a regular crystal lattice prevents crystallization but promotes aggregation.¹⁰ While we do not know the structure of these “soft aggregates” in detail by our measurement of dynamics, these aggregates should be liquidlike enough since they do not bleach. Moreover, the aggregates are transparent and optically isotropic in a sense that we could not directly see them under our optical microscope with or without crossed polarizers.

As a mechanism of the formation of the soft aggregates,

we assume that while the side surface of the needles rejects to incorporate most of the molecules into crystal structure, they can stay attached loosely on the surface for the attraction between molecules. Accumulating these molecules forms eventually softly connected aggregates around the surface.

These soft aggregates can also be a source of the branching of the needlelike crystals forming spherulites. If the soft aggregates act as impurities accumulated around the crystal surface, the instability of the crystal growth can be caused by a well-known Mullins–Sekerka mechanism.¹⁴ When a crystal is growing in an inhomogeneous concentration field of impurities, the fluctuation of the crystal surface is enhanced rather than decayed, if the fluctuation brings the surface into a position where the concentration of impurities is low. In fact, this impurity-driven instability and spherulites formation have been observed in a system of polymer blends.²⁹ Another possibility is that the branching is caused directly by the aggregates. In fact, aggregates (or “liquid-state”) mediated crystallization is observed on the surface of lysozyme crystals using atomic force microscopy.³⁰ If the aggregates change the orientation of the crystal surface slightly, the branching can happen from there.

We note that as seen in Fig. 5(a), there always seems to exist well-stretched needles without branching at the growth front of a spherulite. While they do not experience the instability judging from their shape without branching, they may create soft aggregates around their surface so that the branching occurs behind them, that is, behind the growth fronts of the spherulite.

C. Spherulite maturation

The soft aggregates, or the dense liquid state of the molecules, start to disappear at $t_m \approx 20$ h, as shown in Figs. 5(b) and 5(d). To coincide with the disappearance, the spherulite begins to mature, as shown in Fig. 8(b). While the characteristic crystal size in a spherulite does not change much during the initial stage of crystallization ($t_m < 20$ h), it starts to grow rather suddenly at about $t_m \approx 20$ –30 h, as shown in Fig. 8(b). A combination between this fact and discussion above suggests that the soft aggregates prevent the crystals to mature. This is consistent with the idea that soft aggregates act as impurities to cause instability of the crystal growth.

The disappearance of the soft aggregates allows crystals to start maturing. As the cause of the disappearance, we consider that the internal structure of the spherulites is rather porous and the solution in between needles is exchangeable with the solution outside the spherulite. Thus, when the concentration in solution outside the spherulites decreases below the “solubility” of the soft aggregates due to the crystal growth, they start to dissolve. Since the stability of the soft aggregates is considered to be lower than that of the crystals, their solubility is higher than that of the crystals.

After the disappearance of the aggregates and during the crystal maturation, FCS observes the same diffusion as in bulk solution. This suggests that the crystals can anneal themselves by growing in a dilute solution without any ag-

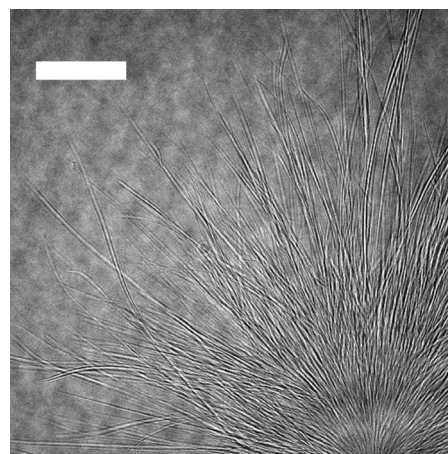


FIG. 10. A micrograph of a spherulite in the same solution used for above measurements, taken 3 weeks after the preparation. The scale bar is 20 μm . There were fully grown needles without branching.

gregates, which is consistent with the fact that the tetragonal single crystals grow without these aggregates.

As an example of the final state of spherulites, we show a micrograph taken 3 weeks after the preparation in Fig. 10. The spherulite was fully grown with stretched needles without branching. The branching stops occurring in the middle of the spherulite. This shows that the branching does not occur in the late stage of the spherulite growth, where no soft aggregates exist. This is consistent with the idea of the aggregates-driven branching.

V. CONCLUSIONS

We applied FCS on protein lysozyme solutions during crystallization, and showed that FCS was useful for the study of protein crystallization since it provided unique information about local molecular dynamics close to crystal surfaces. For tetragonal single crystals, slow dynamics of molecules with the relaxation time several times longer than that in bulk solution probably on the surface was observed where the distance between the observation point and the crystal surface was closer than 1 μm . The origin of this slow dynamics is probably the molecules slowed by the interaction with the surface. The concentration of molecules there was similar to that observed in bulk solution. In short, we did not find any unexpected change in dynamics and concentration profile of molecules close to the tetragonal crystal surfaces.

On the other hand, much slower dynamics with the relaxation time a few orders of magnitude longer than that in bulk solution was observed in needlelike spherulites. Moreover, the concentration there was found to be several times higher than that in bulk solution. From these results, we suggested that there were slowly diffusing and softly connected aggregates around the needlelike crystals, and that these aggregates could cause the branching of the crystals, which could eventually lead to spherulite formation. The aggregates disappeared at the late stage of the crystallization, and crystal maturation started there.

It is not yet clear if these findings can be applied to many other protein systems where spherulitic crystallization occurs. However, considering the tendency for protein mol-

ecules to aggregate, it is possible that the mechanism suggested in this study is one of the origins in general for the crystal branching and spherulite formation in protein solutions.

ACKNOWLEDGMENTS

S.T. thanks Professor A. Toda, Dr. K. Taguchi, Dr. H. Kajioaka, and Dr. R. C. Gosh for a fruitful discussion. This work was supported by KAKENHI (Grant-in-Aid for Scientific Research) on Priority Area "Soft Matter Physics" from the Ministry of Education, Culture, Sports, Science and Technology of Japan.

¹C. Ishimoto and T. Tanaka, *Phys. Rev. Lett.* **39**, 474 (1977).

²B. M. Fine, J. Pande, A. Lomakin, O. O. Ogun, and G. B. Benedek, *Phys. Rev. Lett.* **74**, 198 (1995).

³M. Muschol and F. Rosenberger, *J. Chem. Phys.* **107**, 1953 (1997).

⁴S. Tanaka, M. Yamamoto, K. Ito, R. Hayakawa, and M. Ataka, *Phys. Rev. E* **56**, R67 (1997).

⁵M. C. R. Heijna, M. J. Theelen, W. J. P. van Enkevort, and E. Vlieg, *J. Phys. Chem. B* **111**, 1567 (2007).

⁶J. D. Ng, B. Lorber, J. Witz, A. Théobald-Dietrich, D. Kern, and R. Giegé, *J. Cryst. Growth* **168**, 50 (1996).

⁷S. Tanaka, K. Ito, R. Hayakawa, and M. Ataka, *J. Chem. Phys.* **111**, 10330 (1999).

⁸A. M. Kulkarni, N. M. Dixit, and C. F. Zukoski, *Faraday Discuss.* **123**, 37 (2003).

⁹S. Tanaka, M. Ataka, and K. Ito, *Phys. Rev. E* **65**, 051804 (2002).

¹⁰A. McPherson, *Crystallization of Biological Macromolecules* (Cold Spring Harbor Laboratory, New York, 1999).

¹¹A. C. Dumetz, A. M. Chockla, E. W. Kaler, and A. M. Lenhoff, *Biochim. Biophys. Acta. Proteins Proteomics* **1784**, 600 (2008).

¹²H. D. Keith and J. F. J. Padden, *J. Appl. Phys.* **34**, 2409 (1963).

¹³A. Toda, K. Taguchi, and H. Kajioaka, *Macromolecules* **41**, 7505 (2008).

¹⁴W. W. Mullins and R. F. Sekerka, *J. Appl. Phys.* **34**, 323 (1963).

¹⁵A. Kierzek, P. Pokarowski, and P. Zielenkiewicz, *Biophys. Chem.* **87**, 43 (2000).

¹⁶N. L. Thompson, in *Topics in Fluorescence Spectroscopy*, Techniques Vol. 1, edited by J. R. Lakowicz (Plenum, New York, 1991).

¹⁷P.-O. Gendron, F. Avaltroni, and K. J. Wilkinson, *J. Fluoresc.* **18**, 1093 (2008).

¹⁸W. Eberstein, Y. Georgalis, and W. Saenger, *J. Cryst. Growth* **143**, 71 (1994).

¹⁹P. Retailleau, M. Ries-Kautt, A. Ducruix, L. Belloni, S. Candau, and J. Munch, *Europhys. Lett.* **46**, 154 (1999).

²⁰Y. Saito, *Statistical Physics of Crystal Growth* (World Scientific, Singapore, 1996).

²¹T. Nakada, G. Sazaki, S. Miyashita, S. D. Durbin, and H. Komatsu, *J. Cryst. Growth* **196**, 503 (1999).

²²A. Malkin, Y. Kuznetsov, and A. McPherson, *J. Cryst. Growth* **196**, 471 (1999).

²³A. E. S. van Driessche, G. Sazaki, G. Dai, F. Otalora, J. A. Gavira, T. Matsui, I. Yoshizaki, K. Tsukamoto, and K. Nakajima, *Cryst. Growth Des.* **9**, 3062 (2009).

²⁴A. A. Chernov, *Modern Crystallography III* (Springer-Verlag, Berlin, 1984).

²⁵G. Sazaki, M. Okada, T. Matsui, T. Watababe, H. Higuchi, K. Tsukamoto, and K. Nakajima, *Cryst. Growth Des.* **8**, 2024 (2008).

²⁶V. Ball and J. Ramsden, *Biopolymers* **46**, 489 (1998).

²⁷P. R. ten Wolde and D. Frenkel, *Science* **277**, 1975 (1997).

²⁸P. Vekilov, *Cryst. Growth Des.* **4**, 671 (2004).

²⁹H. Tanaka and T. Nishi, *Phys. Rev. Lett.* **55**, 1102 (1985).

³⁰Y. Kuznetsov, A. Malkin, and A. McPherson, *Phys. Rev. B* **58**, 6097 (1998).